Electronic supplementary information

Pollen-derived porous carbon decorated with cobalt/iron sulfides hybrids as cathode catalyst for robust flexible all-solid-state rechargeable Zn-air battery

Weiguang Fang [a, b, c], Zhiman Bai [a, c], XinxinYu [a, c], Wen Zhang [a, c], Mingzai Wu [a, c, *]

Materials characterization

Scanning electron microscopy (SEM) images, energy dispersive spectrums (EDS) and elemental mappings of samples were conducted on a Hitachi Regulus8230 field-emission ultra-high resolution scanning electron microscope. Transmission electron microscopy (TEM) images and high-resolution transmission electron microscopy (HRTEM) images of samples were carried out using a JEOL JEM-2100 high resolution-transmission electronic microscope. Powder X-ray diffraction (XRD) patterns of samples were performed using a Rigaku smart Lab X-ray diffractometer with Cu K_α radiation. Raman spectra of samples were investigated with inVia-Reflex confocal laser

---

[a] School of Physics and Materials Science, Anhui University, Hefei, 230601, China. *E-mail: wumz@ahu.edu.cn*

[b] College of Chemistry and Chemical Engineering, Hefei Normal University, Hefei, 230601, China

[c] Key Laboratory of photoelectric conversion energy materials and devices of Anhui Province, Key Laboratory of hybrid material structure and function regulation, Ministry of Education, Anhui University, Hefei, 230601, China

micro-Raman spectrometer. The N_2 adsorption-desorption isotherm of samples were performed using a BeiShiDe 3H-2000PS2 instrument at 77 K. The special surface areas and the pore size distributions of samples were calculated by the Brunauer-Emmett-Teller (BET) method and fitted by the Barrett-Joyner-Halenda (BJH) model, repectively. X-ray photoelectron spectroscopy (XPS) spectra of samples were conducted on ESCALAB 250Xi X-ray photoelectron spectrometer with Mg Kα achromatic X-ray source.

Electrochemical measurements

The electrochemical tests were performed at room tempture using a Chenhua CHI 660E electrochemical work station with three electrode system in 0.1 M KOH aqueous solution electrolyte. An Ag/AgCl electrode and a Pt wire were served as the reference electrode and the counter electrode, respectively. A Pine rotating disk electrode (RDE, the surface area of the disk is 0.1962 cm^2) or rotating ring-disk electrode (RRDE, the surface area of the disk is 0.2475 cm^2, the surface area of the ring is 0.1866 cm^2) with 0.39 $mg\cdot cm^{-2}$ or 0.31 $mg\cdot cm^{-2}$ catalyst loading was used as the working electrode. The catalyst was loaded on the working electrode in ink liquid form (8 μL), which was prepared by sonicating the solution containing 5 mg of catalyst, 350 μL of deionized water, 150 μL of isopropanol, 25 μL of 5wt % Nafion solutions, and then was dried under room temperature. All the measured potentials in this work were converted against the reversible hydrogen electrode (RHE) according to the Nernst equation ($E_{RHE} = E_{Ag/AgCl} + 0.059\ pH + E^{\theta}_{Ag/AgCl}$). The cyclic voltammetry (CV) measurements of samples were carried out at a scan rate of 20 mV s^{-1} in O_2 or N_2-saturated electrolyte.

The ORR performance of samples were performed by using the linear sweep voltammetry (LSV) technique after iR correction at a scan rate of 10 mV·s^{-1} in O_2-saturated electrolyte with different rotation rates from 400 to 2500 rpm. The number of electrons transferred by each oxygen atom in ORR was calculated based on the Koutecky-Levich (K-L) equation,

$$\frac{1}{j}=\frac{1}{j_k}+\frac{1}{j_L}=\frac{1}{j_k}+\frac{1}{B\omega^{-1/2}} \tag{1}$$

$$B = 0.62nFC_oD_o^{2/3}\upsilon^{-1/6} \tag{2}$$

$$j_k= nFkC_o \tag{3}$$

Where n is the calculated number of transferred electrons, ω is the disk rotation rate of the RDE, C_o is the saturated oxygen concentration in 0.1 M KOH electrolyte, D_o is the diffusion coefficient of oxygen (1.9 × 10^{-5}·cm^2·s^{-1}), υ is the kinematic viscosity of the 0.1 M KOH electrolyte (0.01 cm^2·s^{-1}), F is the Faradic constant (96485 C mol^{-1}), and k is the electron transfer rate constant.

The RRDE measurement was also be applied to detect the percentage of intermediate production (HO^{2-} %) and to determine the electron transfer number (n) of catalyst in ORR base on the following equations,

$$HO^{2-}\% = 200\frac{I_{ring}/N}{I_{disk}+I_{ring}/N} \tag{4}$$

$$n = 4\frac{I_{disk}}{I_{disk}+I_{ring}/N} \tag{5}$$

where I_{disk} and I_{ring} represent current of the disk and the ring, respectively, and N denotes the current collection efficiency of the RRDE (0.37).

The OER performances of samples were performed by LSV measurement at a scan rate of 10 mV s^{-1} with iR-corrected. The OER reaction order can were determined on the slopes the fitted linear portion of the Tafel plots from the corresponding LSV curves. The Tafel slopes of LSV curves for OER were determined on the fitted linear portion of the Tafel plots ($\eta = a + b \log|j|$, where η, b and j are denote the overpotential, Tafel slope and current density, respectively.). The electrochemically active surface areas (ECSA) of samples were estimated by the double-layer capacitance (C_{dl}) method in O_2-saturated 0.1M KOH electrolyte. The corresponding C_{dl} values are calculated via the following equation:

$$C_{dl} = \frac{i}{v} \tag{6}$$

Where i represents current density and v represents the scan rate of the scan-rate-dependent CV curves.

The electrochemical impedance spectroscopy (EIS) were measured by using an AC with a 10 mV amplitude over frequency range from 100,000 to 1 Hz and recorded at 0 V (vs. Ag/AgCl).

Zn-air battery measurements

Discharge and charge performance of liquid ZAB was test by LSV technique at a scan rate of 10 mV s^{-1} on a Chenhua CHI 660E electrochemical work station in ambient atmosphere. The galvanostatic discharge and charge-discharge cycling (10 min charge and 10 min discharge) were recorded by using a LAND testing system at a current density of 10 mA cm^{-2}. The specific capacity and the energy density were calculated normalized to the mass of the consumed zinc according the following equations,

$$Specific\ capacity = \frac{Current \times Discharge\ time}{Weight\ of\ comsumed\ Zn} \tag{6}$$

$$Energy\ density = \frac{Current \times Discharge\ time \times Average\ discharge\ voltage}{Weight\ of\ comsumed\ Zn} \tag{7}$$

The measurements of the home-made flexible all-solid-state ZAB were the same with the above liquid ZAB, except for the current density was changed from 10 mA cm^{-2} to 5 mA cm^{-2} in the galvanostatic discharge and charge-discharge tests.

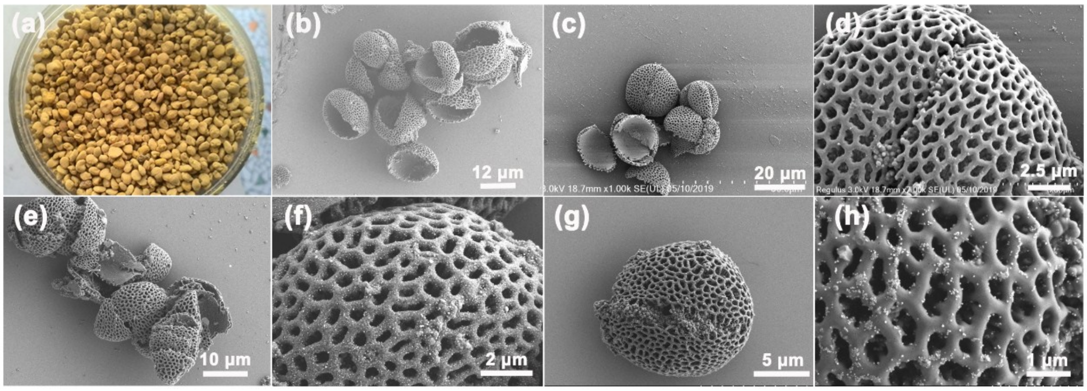

Fig. S1. (a) Photograph of rape pollen; (b) SEM image of Co-Fe-S@NSRPC; (c) SEM image and (d) the enlarged SEM image of NSRPC; (e) SEM image and (f) the enlarged SEM image of Co_9S_8@NSRPC; (g) SEM image and (h) the enlarged SEM image of $Fe_{0.96}S$@NSRPC.

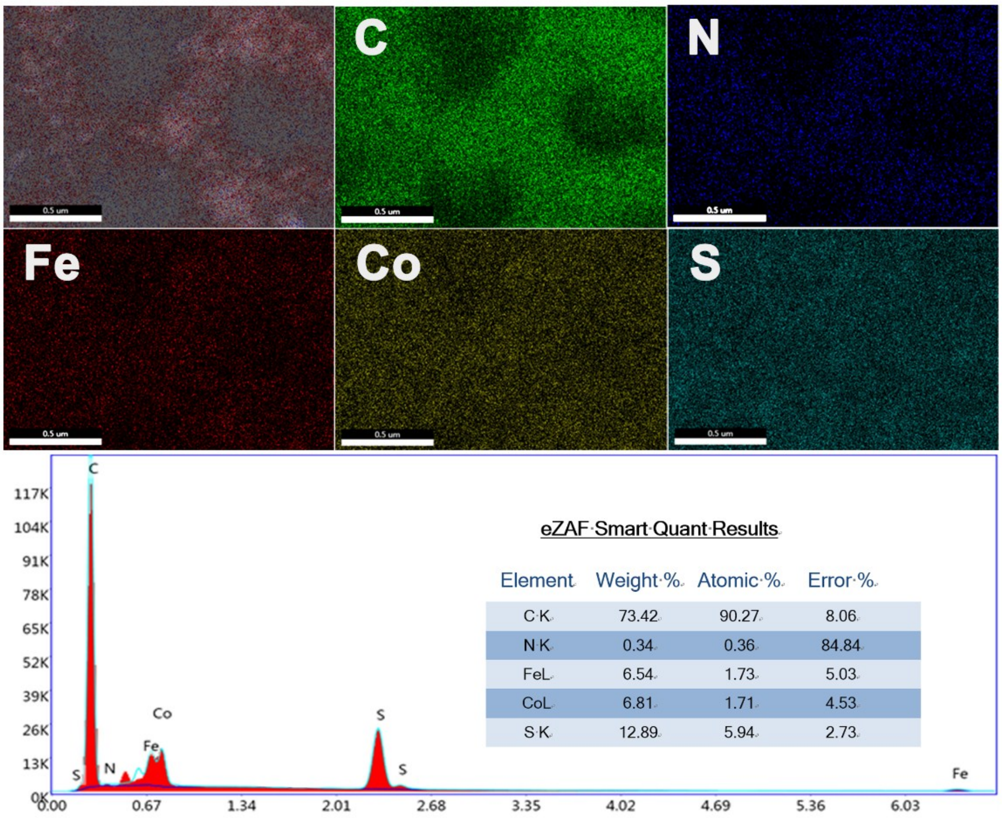

eZAF Smart Quant Results

Element	Weight %	Atomic %	Error %
C K	73.42	90.27	8.06
N K	0.34	0.36	84.84
FeL	6.54	1.73	5.03
CoL	6.81	1.71	4.53
S K	12.89	5.94	2.73

Fig. S2. EDS mapping images and EDS analysis of elements contained in Co-Fe-S@NSRPC characterized by SEM.

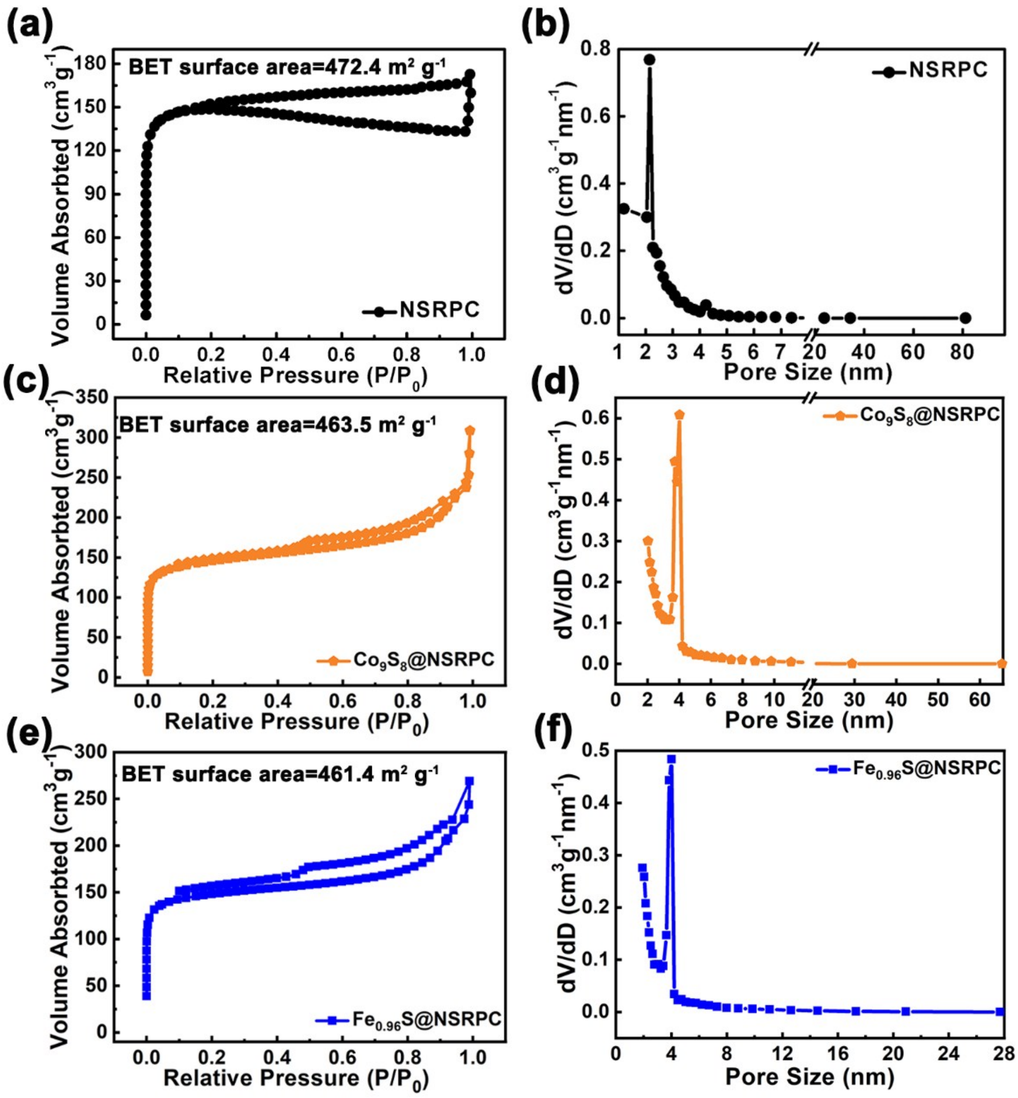

Fig. S3. (a, c, e) N_2 adsorption-desorption isotherm and (b, d, f) BJH pore-size distribution of NSRPC, Co_9S_8@NSRPC and $Fe_{0.96}S$@NSRPC, respectively

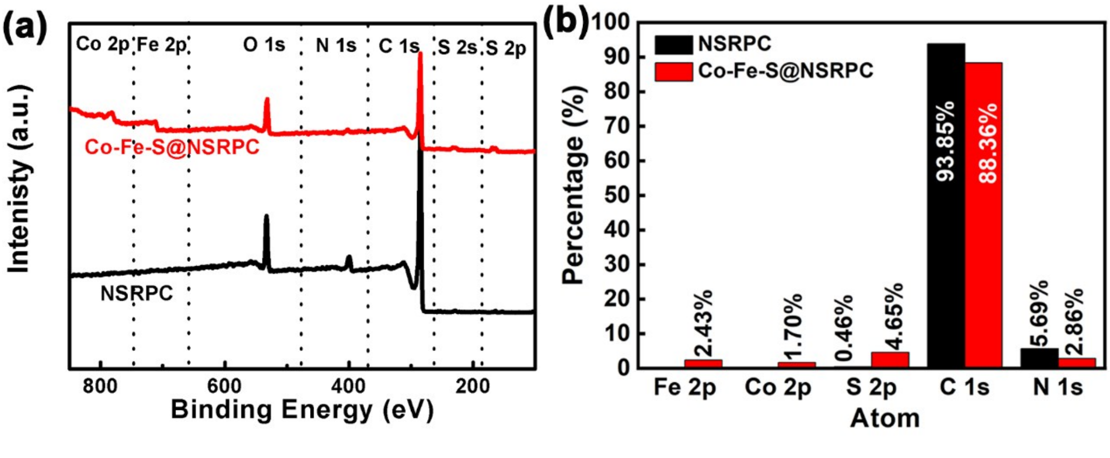

Fig. S4. Comparative XPS survey spectra (a) and atomic percentages cartogram (b) of NSRPC and Co-Fe-S@NSRPC

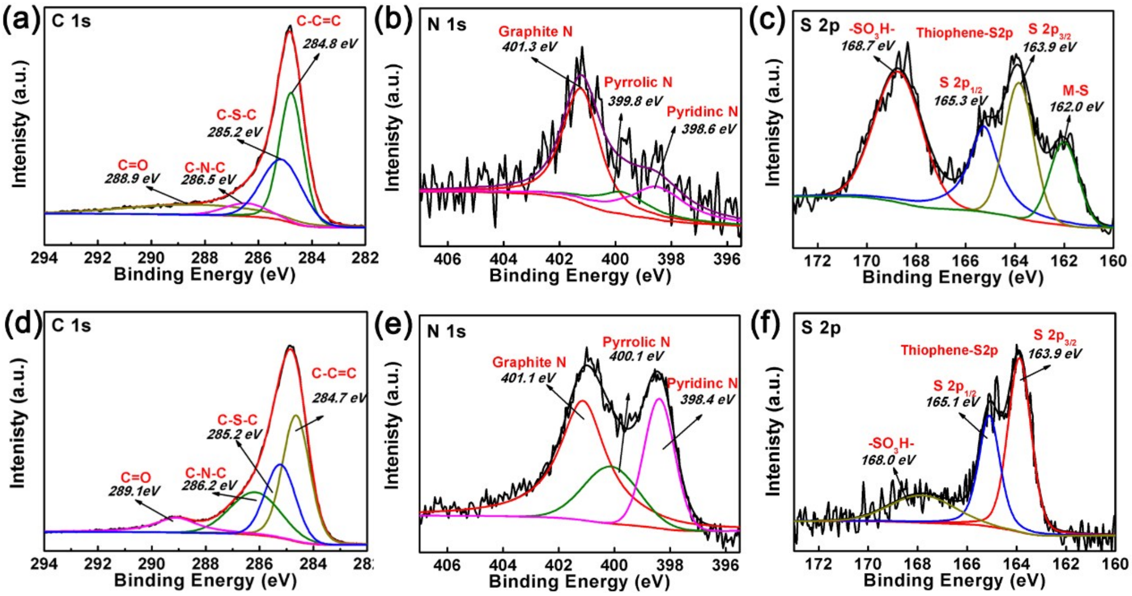

Fig. S5. The high-resolution spectrums of C1s, N1s and S2p in Co-Fe-S@NSRPC (a-c) and NSRPC (d-f).

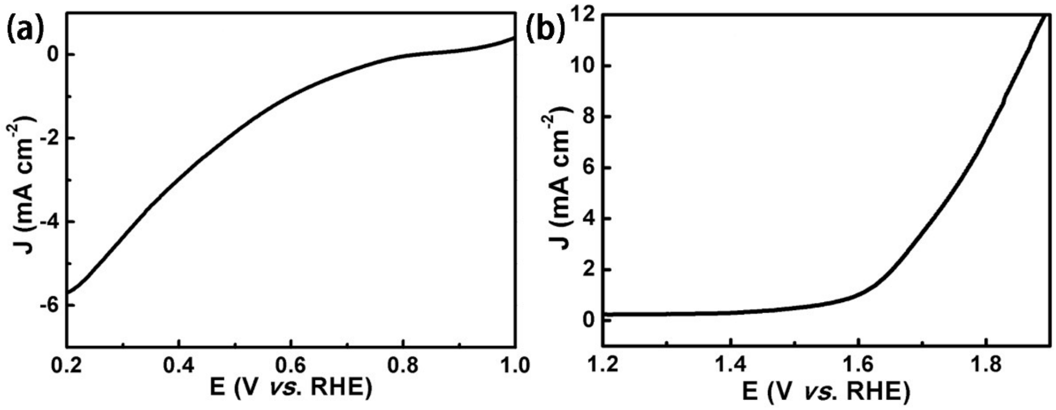

Fig. S6. LSV curves of the Co-Fe-S catalyst for (a) ORR and (b) OER at 5 mVs^{-1} with a rotating rate of 1600 rpm in 0.1 M KOH.

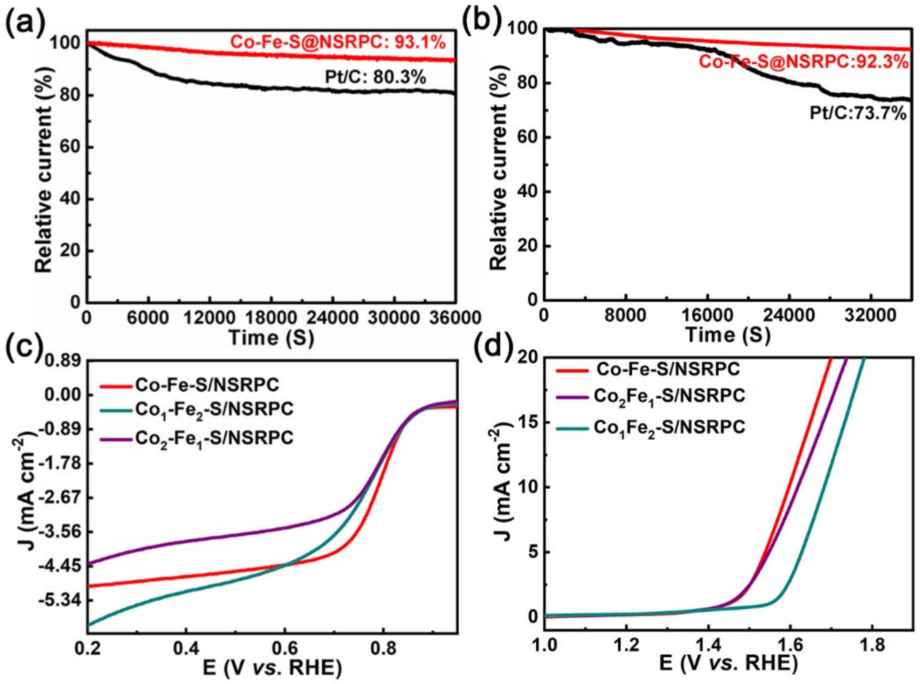

Fig. S7. (a) Chronoamperometric responses (i-t) of ORR on Co-Fe-S@NSPC and 20wt % Pt/C at the same applied potential of 0.80 V over 36000s in O_2-saturated 0.1 M KOH solution; (b) Chronoamperometric responses (i-t) of OER on Co-Fe-S@NSPC and RuO_2 at the same applied potential of 1.60 V over 36000s in O_2-saturated 0.1 M KOH solution. (c) ORR and (d) OER LSV curves of the catalysts of Co-Fe-S@NSRPC, Co_1Fe_2-S@NSRPC and Co_2Fe_1-S@NSRPC, which were prepared with the amount ratio of $Fe(NO_3)_3 \cdot 9H_2O$ and $Co(NO_3)_2 \cdot 6H_2O$ introduced in the preparation process of 0.2:0.2, 0.15:0.3 and 0.3:0.15, respectively.

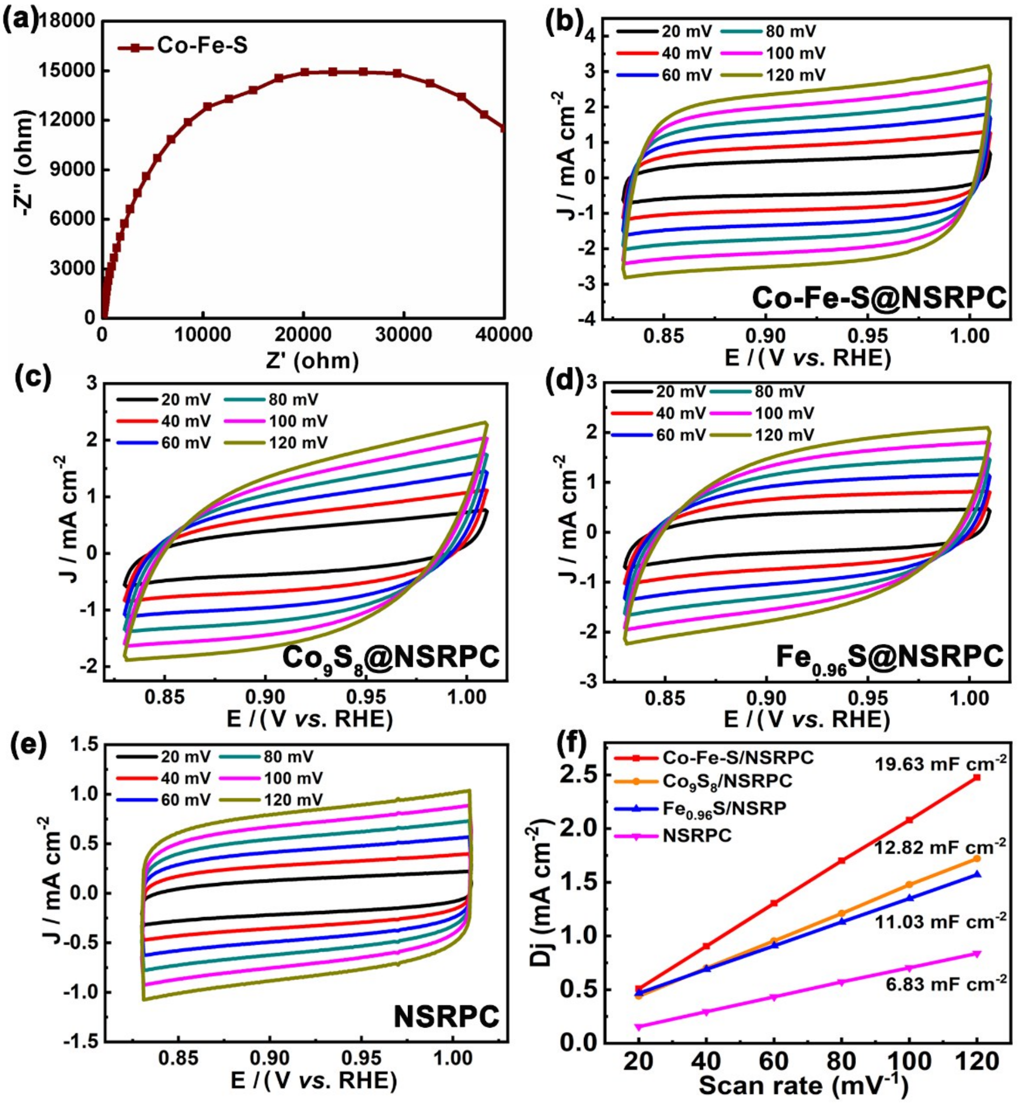

Fig. S8. (a) Nyquist plots of Co-Fe-S (vs. Ag/AgCl) with frequency from 100000 Hz to 0.01 Hz with an AC voltage amplitude of 5 mV in 0.1 M KOH solution; (b-e) CVs at different scan rates from 20 to 120 mV s^{-1} in 1.0 M KOH, and (f) the corresponding C_{dl} of Co-Fe-S@NSPRC, Fe$_{0.96}$S@NSRPC, Co$_9$S$_8$@NSRPC, NSRPC.

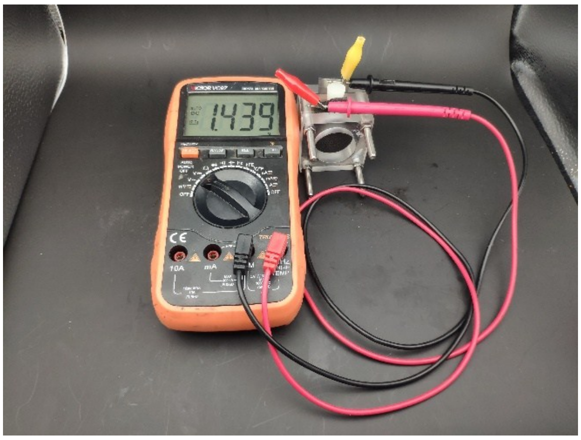

Fig. S9. The photograph illustrates the open-circuit voltage of ZAB based on Pt/C + RuO$_2$.

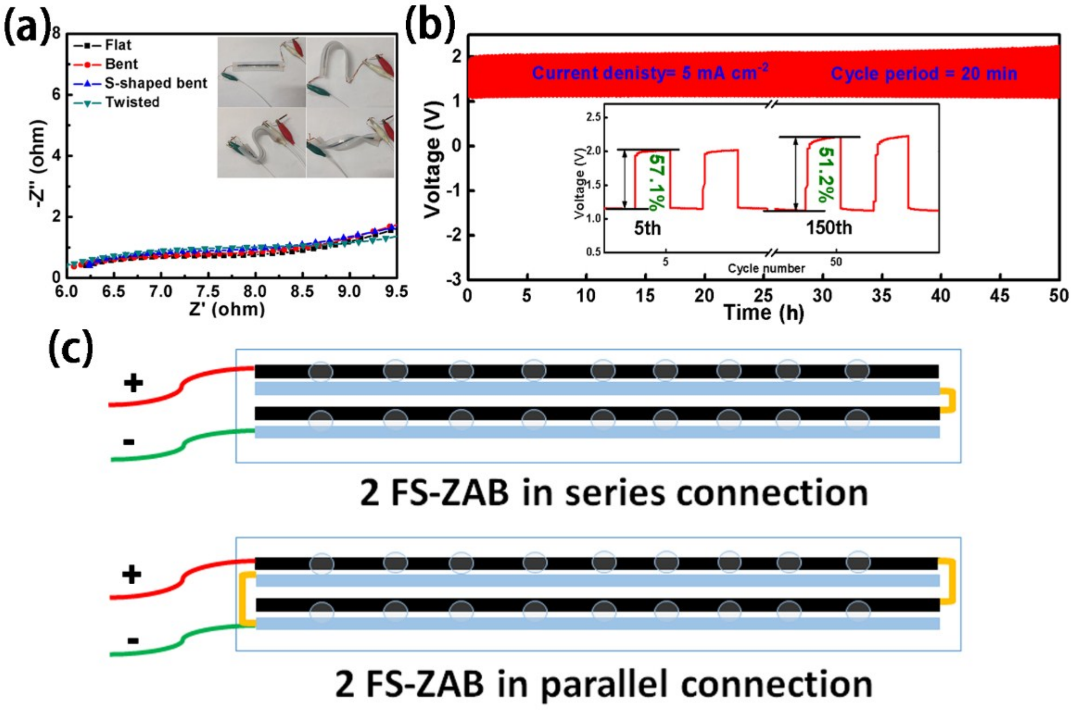

Fig. S10. (a) Nyquist plots of the flat, bent, S-shaped bent and twisty FS-ZAB based on Co-Fe-S@NSRPC cathode catalyst with frequency from 100000 Hz to 0.01 Hz at an AC voltage amplitude of 5 mV, respectively. (Inset is the simplified Randles equivalent circuit); (b) The galvanostatic charge-discharge cycling curve of FS-ZAB at 5 mA cm^{-2}; (c) The abridged general views of integrated units with 2 FS-ZAB in series connection and with 2 FS-ZAB in parallel connection, respectively.

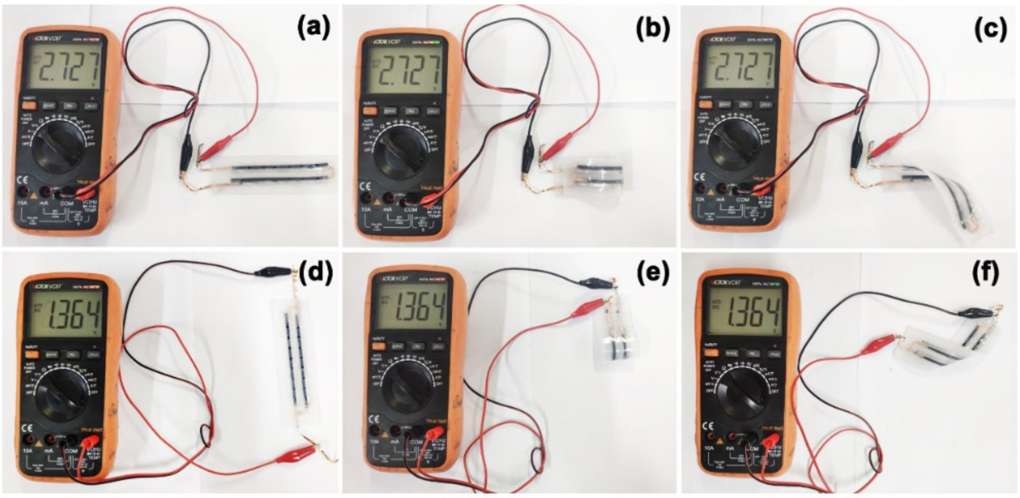

Fig. S11. Photographs of the open-circuit voltages of integrated units with 2 FS-ZAB in series connection (a-c) and with 2 FS-ZAB in parallel connection (d-f) at different bending angles, respectively.